

JGR Oceans

RESEARCH ARTICLE

10.1029/2024JC021337

Key Points:

- Kuroshio intrusion alleviates nearshore phosphorus limitation and supports spring and summer algal blooms
- The phytoplankton community composition and biomass are largely regulated by temperature, salinity, N/P ratio and DIP
- Kuroshio intrusion transports oceanic warm-water species that increases phytoplankton diversity

Supporting Information:

Supporting Information may be found in the online version of this article.

Correspondence to:

Z. Jiang and Q. Chen, jzb@sio.org.cn; chenqz6509@126.com

Citation:

Sun, Z., Zhu, Y., Jiang, Y., Zhai, H., Chen, J., Yan, X., et al. (2025). Intrusion of kuroshio enhances phytoplankton biomass and diversity in the East China Sea. *Journal of Geophysical Research: Oceans*, 130, e2024JC021337. https://doi.org/10.1029/2024JC021337

Received 16 MAY 2024 Accepted 6 FEB 2025

Author Contributions:

Data curation: Zhenhao Sun Formal analysis: Jianfang Chen Funding acquisition: Zhibing Jiang Investigation: Yulu Jiang, Quanzhen Chen

Methodology: Yuanli Zhu, Xiaojun Yan Project administration: Quanzhen Chen Resources: Hongchang Zhai,

Quanzhen Chen
Software: Zhenhao Sun, Yuanli Zhu

Supervision: Jiangning Zeng, Zhibing Jiang

Visualization: Zhenhao Sun Writing – original draft: Zhenhao Sun Writing – review & editing:

Zhibing Jiang

© 2025. American Geophysical Union. All Rights Reserved.

Intrusion of Kuroshio Enhances Phytoplankton Biomass and Diversity in the East China Sea

Zhenhao Sun^{1,2} D, Yuanli Zhu^{1,3} D, Yulu Jiang¹, Hongchang Zhai¹, Jianfang Chen^{1,2,4} D, Xiaojun Yan⁵, Jiangning Zeng^{1,2,3,4} D, Quanzhen Chen¹ D, and Zhibing Jiang^{1,3,4,6}

¹Key Laboratory of Marine Ecosystem Dynamics, Second Institute of Oceanography, Ministry of Natural Resources, Hangzhou, China, ²School of Oceanography, Shanghai Jiao Tong University, Shanghai, China, ³Key Laboratory of Nearshore Engineering Environment and Ecological Security of Zhejiang Province, Hangzhou, China, ⁴State Key Laboratory of Satellite Ocean Environment Dynamics, Second Institute of Oceanography, Ministry of Natural Resources, Hangzhou, China, ⁵Marine Science and Technology College, Zhejiang Ocean University, Zhoushan, China, ⁶Observation and Research Station of Marine Ecosystem in the Yangtze River Delta, Ministry of Natural Resources, Hangzhou, China

Abstract The Kuroshio, the North Pacific Ocean's most robust western boundary current, brings a rich infusion of nutrients (especially phosphate) and warm-water species into the East China Sea (ECS), profoundly shaping its environmental conditions and ecological processes. However, the precise impact of Kuroshio intrusion on the composition and distribution of phytoplankton communities remains unclear. We hypothesized that the Kuroshio intrusion alleviates phosphorus limitations on phytoplankton growth and enhances phytoplankton diversity within the ECS. We collected phytoplankton samples and relevant physicochemical data from the ECS across four seasons in 2011. We observed that phytoplankton abundance and chlorophyll a concentration were significantly higher during summer and autumn compared to winter and spring. Notably, elevated phytoplankton biomass was detected in the Zhejiang coastal waters during spring, and along the boundary between Kuroshio Subsurface Water and Changjiang Diluted Water during summer and autumn. The dissolved inorganic phosphorus (DIP) carried by Kuroshio subsurface water mitigated the phosphorus limitation in summer and stimulated the growth of phytoplankton in spring and autumn. Redundancy analysis revealed a strong association between low-salinity species and nutrient levels, while warm-water species appeared to be influenced primarily by temperature. Generalized additive models further elucidated that phytoplankton biomass in coastal region was primarily influenced by nitrogen/phosphorus (N/P) ratio, and silicate/nitrogen (Si/ N) ratio, whereas in Kuroshio region, DIP and N/P ratio played more significant roles. In mixed region, phytoplankton biomass was influenced by temperature, Si/N ratio, and stratification. The intrusion of the Kuroshio significantly enhanced phytoplankton diversity (species number, warm-water species number, and Shannon index) in the Kuroshio region compared to the coastal and mixed regions. These findings underscore the substantial influence of Kuroshio intrusion on the spatial and seasonal variations of phytoplankton biomass and community composition within the ECS.

Plain Language Summary The Kuroshio, a powerful ocean current in the North Pacific, carries abundant phosphate and warm-water species into the ECS, profoundly impacting its environment and ecosystems. We hypothesize that Kuroshio intrusion into the ECS promotes phytoplankton growth by alleviating phosphorus limitations and enhances phytoplankton diversity through the transportation of warm-water species from the ocean. To test this hypothesis, we conducted four cruises in the ECS throughout the four seasons of 2011, collecting data on phytoplankton communities and physicochemical properties. Our results indicate that phosphate carried by the Kuroshio intrusion promotes phytoplankton growth, while the influx of warm-water species and heat enhances phytoplankton diversity in the ECS.

1. Introduction

The ocean circulation system can cause ocean water to infiltrate coastal regions, impacting the characteristics and ecological processes of marginal seas (Kobayashi & Fujiwara, 2008). The Kuroshio, the most potent western boundary current in the North Pacific Ocean, originates from the northern branch of the Northern Equatorial Current in the eastern Philippine Sea. It enters the East China Sea (ECS) via the northeast of Taiwan Island and the southwest of the Ryukyu Islands (Qu et al., 2016). According to Yang et al. (2018), a nearshore Kuroshio Branch Current (NKBC) originating from the Kuroshio Subsurface Water (KSSW) is observed from April to July.



Moreover, during summer, the mainstream of the Kuroshio deflects toward the shore, leading to intensified NKBC shoreward intrusion, and carrying significant amounts of phosphate and warm-water species into the ECS (Wang et al., 2018; Zhang et al., 2007). Kondo (1985) observed Kuroshio intrusions from the northeast of Taiwan occurring throughout the year. Influenced by temperature changes, the Kuroshio Surface Water (KSW), with relative oligotrophication and high temperature and high salinity, deflects toward the continental shelf in winter (Oey et al., 2010). Consequently, there is differential enhancement of KSW and KSSW between warm and cold seasons: KSW intrudes into the ECS during winter and autumn, while KSSW strongly penetrates the ECS and approaches coastal waters near 30°N in summer (Wu et al., 2014; Yang et al., 2011, 2012). The Kuroshio and its branches are recognized as the primary factors shaping ECS circulation and profoundly influencing phytoplankton community structure (Jiang et al., 2014, 2015).

Nutrients play a pivotal role in driving phytoplankton growth and primary productivity, with coastal regions often experiencing severe phosphorus limitations (Trommer et al., 2013; Wang et al., 2021; Yu & Gan, 2022). While phytoplankton growth typically adheres to the Redfield ratio, the N/P ratio carried by the Changjiang Diluted Water (CDW) far exceeds 16 (often reaching around 100), leading to phosphorus deficiency and hindering phytoplankton growth (Chen et al., 2004; Gong et al., 1996; Harrison et al., 1990; Li et al., 2009; Tseng et al., 2014). The phosphates transported by the Kuroshio can alleviate this phosphorus limitation in the ECS, potentially influencing phytoplankton abundance and community composition (Tseng et al., 2014; Zhang et al., 2007). Furthermore, warm-water species like *Trichodesmium*, carried by the Kuroshio, may significantly alter phytoplankton species composition in the ECS (Jiang et al., 2018). Previous research indicates that Kuroshio intrusion into the ECS regulates distribution and community structure, enhancing the diversity of benthic fishes (Y. Xu et al., 2019), macrofauna (Xu et al., 2018), and radiolarians (Qu et al., 2020). Zhao et al. (2019) demonstrated that the distribution of pico-phytoplankton Prochlorococcus reflects the intrusion path of the NKBC, with the Kuroshio's transport significantly influencing the dynamics of harmful algal blooms (HABs) in the region. Additionally, the Taiwan Warm Current (TWC), formed by the mixing of Taiwan Strait water and intruding Kuroshio water, flows northward, impacting heat, salinity, and nutrient balance in the ECS (Chen, 2009; Jiang, Chen, Zhai, et al., 2019; Lian et al., 2016). Consequently, the significant intrusion of the Kuroshio and its branches into the ECS can profoundly affect the community composition and biomass of phytoplankton.

Previous studies have primarily focused on coastal waters such as the Changjiang Estuary (CE) or the ECS in individual seasons (Jiang et al., 2014, 2015; Wu et al., 2000). Few have explored variations in phytoplankton communities across all seasons in the ECS (Guo et al., 2014), and even fewer have specifically addressed the impact of Kuroshio intrusion. Moreover, most research has centered on the effects of CDW on phytoplankton composition and distribution in the CE (Jiang et al., 2014, 2015; Zhou et al., 2012), with limited investigations into the influence of Kuroshio intrusion on seasonal and spatial changes in phytoplankton communities. Consequently, the extent to which Kuroshio intrusion shapes the composition and distribution of phytoplankton communities in the ECS remains uncertain. Here, we propose that Kuroshio intrusion into the ECS promotes phytoplankton growth by alleviating phosphorus limitations and enhances phytoplankton diversity through the transportation of warm-water species from the ocean. To test this hypothesis, we conducted four cruises in the ECS (26°-33°N, 121°-128°E) across four seasons of 2011, collecting data on phytoplankton community characteristics (abundance, chlorophyll a concentration, group composition, dominant species, and diversity) and physicochemical properties. By analyzing the temporal and spatial variations of the Kuroshio, we investigated its influence on the composition and distribution of phytoplankton communities in the ECS. These findings offer valuable insights into the temporal and spatial distribution and community structure of phytoplankton in the ECS under the influence of Kuroshio intrusion, laying a foundation for understanding the broader impacts of this intrusion on the ECS ecosystem.

2. Materials and Methods

2.1. Study Area and Sampling Strategies

Four multidisciplinary cruises were conducted in the ECS for four seasons of 2011 by the research vessel *Dongfanghong 2#*. A total of 46, 35, 41, and 46 sampling stations were arranged in the study area (121.0–127.5°E, 26.5–33°N; Figure 1) in winter, spring, summer, and autumn, respectively. At each station, water temperature, salinity, and depth were measured using a conductivity-temperature-depth (CTD) recorder (SBE 917 Plus, SeaBird, Sea Bird Corporation, USA). Water samples were collected at various depths (3, 10, 30, 50, 75, 100, 150,

SUN ET AL. 2 of 17

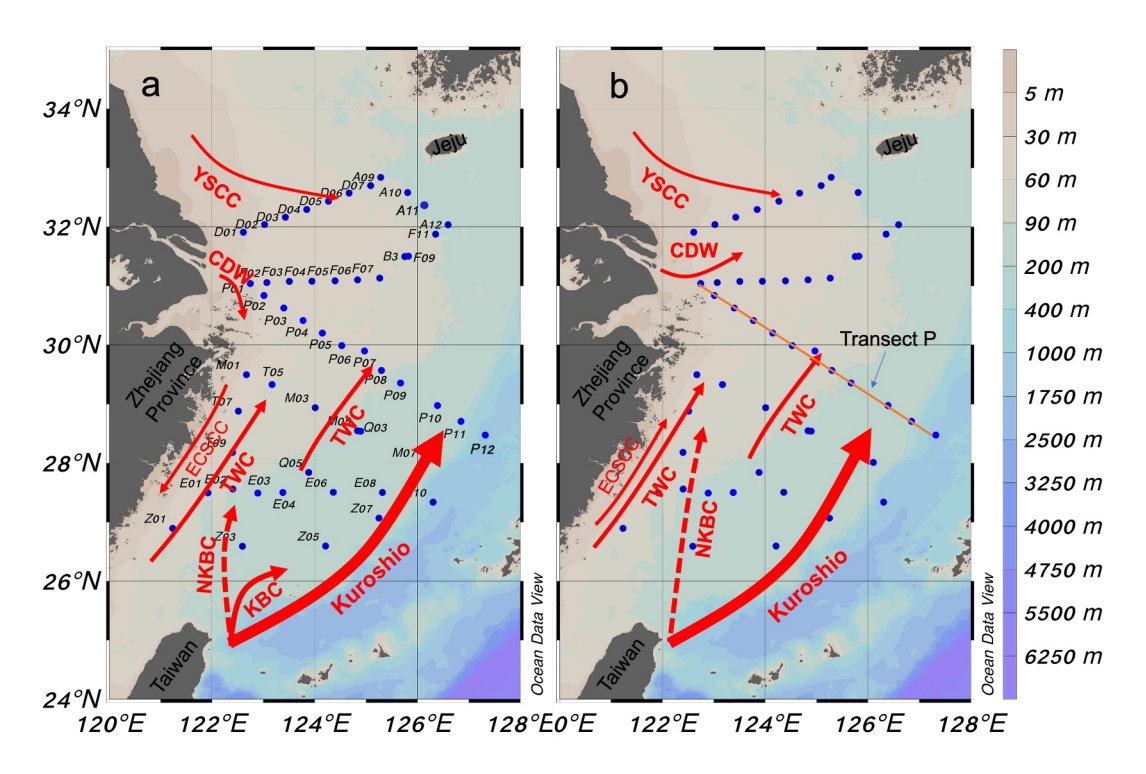


Figure 1. Sampling stations and a schematic showing winter (a) and summer (b) circulation (according to Bian et al., 2013) in the ECS. YSCC, Yellow Sea Coastal Current; CDW, Changjiang Diluted Water; TWC, Taiwan Warm Current; NKBC, Nearshore Kuroshio Branch Current; KBC, Kuroshio Branch Current; ECSCC, ECS Coastal Current.

and 200 m, as well as the bottom) using 12-L Niskin bottles. Analysis of dissolved inorganic nitrogen (DIN: NH_4^+ , NO_3^- and NO_2^-), dissolved inorganic phosphorus (DIP), and dissolved silicate (DSi) was conducted using a continuous-flow analyzer (Skalar San⁺⁺, Netherlands) after filtration through a 0.45 µm polycarbonate membrane. Chlorophyll a concentrations were determined from 100 mL seawater samples filtered through GF/F filters, utilizing a Turner Design Fluorometer. GF/F filters were soaked in 90% acetone, and pigments were extracted for 24 hr at -20° C in darkness before subsequent fluorometric evaluation. The temperature, salinity, nutrient, and chlorophyll a data sets used in this analysis have already been published (Jiang et al., 2018).

Phytoplankton samples (1 L) were collected from Niskin bottles at different depths, then preserved in 2% neutral formalin immediately. After quiescence in the laboratory for 24 hr, phytoplankton samples were concentrated using an 8-µm nylon membrane, then rinsed the filter membrane from top to bottom with pure water and drew the concentrated phytoplankton sample with a Graduated Polyethylene Transfer Pipette (Thomas Scientific, New Jersey). Repeat the above operations 2–3 times. The concentrated samples were transferred to a 1-mL scaled slide for microscopic examination using a Leica DM300B microscope. Phytoplankton biomass was indicated by chlorophyll *a* concentration. Transect P was selected as a contrast in the area affected by the KSSW.

2.2. Statistical Analysis

Using the equation as follows to calculate the depth-integrated densities (DIDs) of phytoplankton (A_t) at each station (Jiang, Chen, Gao, et al., 2019).

$$A_{t} = \left[\sum_{i=1}^{n-1} \frac{(A_{i} + A_{i+1})}{2} \times (D_{i+1} - D_{i}) \right]$$
 (1)

where A_i is the abundance (cells/m³) of the *i*th layer, D_i is the depth (m) of the *i*th layer, n is the number of the sampling layers.

SUN ET AL. 3 of 17



Using the equation as follows to calculate the Shannon index (H) of the phytoplankton community at each station (Shannon, 1948).

$$H = \left[-\sum_{i}^{S} P_{i} \times \ln P_{i} \right] \tag{2}$$

where S is the species richness, P_i is the proportion of individuals of species i, and ln is the natural logarithm.

The top 10 most abundant species were defined as the dominant species. Environmental factors were analyzed using Kruskal-Wallis tests to reveal the differences between seasons, and Spearman's rank correlation assessed the relationship between phytoplankton abundance and environmental variables using SPSS 29.0. The distribution of environmental variables, and phytoplankton abundance of diatom, dinoflagellate, and DIDs was drawn by using Ocean Data View (ODV) 5.6.5. Multidimensional scaling (MDS) and cluster analysis were performed using PRIMER 6.0 to reveal spatial patterns in the community structure, and phytoplankton abundance of species were transformed by log(x+1) and standardized before estimating Bray-Curtis similarities between sample pairs (Clarke & Gorley, 2006). Redundancy analysis (RDA) was performed using CANOCO 5.0 to reveal the linear correlation between environmental factors as explanatory variables and phytoplankton community structure as response variables in the ECS under the intrusion of Kuroshio, and was applied on log(x+1)-transformed dominant phytoplankton species abundance and environmental data. The percentage of variation in phytoplankton dominant species explained by environmental factors was calculated using forward selection. The study area was clustered into three regions based on the temperature and salinity of the upper 30 m water column at each station: coastal region (Green solid square in Figure S1 of Supporting Information S1), mixed region (Blue solid circle in Figure S1 of Supporting Information S1), and Kuroshio region (Red solid triangle in Figure S1 of Supporting Information S1) to compare the influence of Kuroshio intrusion on phytoplankton communities in different regions. The stratification index (SI) of the water column was defined as $\Delta \sigma t = \text{bottom density} - \text{surface}$ density.

The generalized additive models (GAMs) were used to estimate the relative importance of environmental variables in variation in abundances of phytoplankton and chlorophyll a concentration in four seasons using R Studio (version 2023.12.1.402). The abundance of phytoplankton and chlorophyll a was transformed by log(x+1). Variance inflation factor (VIF) was used to analyze the collinearity of the predictors, and environmental factors with VIF greater than 10 were excluded. In order to avoid overfitting of the GAMs, select the one with the smallest Akaike Information Criterion (AIC) value in the GAMs. VIF was established using the car package (version 3.1.2). GAMs were established using the mgcViz package (version 4.3.2).

3. Results

3.1. Physicochemical Variables

The Kruskal-Wallis test revealed significant (p < 0.01) temporal and spatial variations in physicochemical variables in the ECS. Sea surface temperature (SST) exhibited a gradual increase from nearshore to offshore areas across all seasons, with low and high values observed near the CE and in the southeast of the ECS, respectively (Figures 2a–2d). Bottom temperature increased from the CE toward the southeast of the ECS during winter (Figure 2i), with a warm-water tongue evident in the southern ECS (Figure 2j). Conversely, SSS in the CE was notably lower (<28) in summer and autumn due to freshwater input from the CDW. In spring and summer, a northward tongue of water with a salinity of 34 was evident at the bottom (Figures 2m–2p). Figure 2j shows a warm-water tongue in the south ECS in spring and strengthened in summer, resulting in the bottom temperature approaching 20°C.

In summer, a water mass with elevated salinity (>34.4) and high dissolved inorganic phosphorus (DIP) concentration (>4.5 μ mol/L) was observed at the bottom along transect *P* (Figures 3g and 3k). Figures 3k and 3s indicate that the nearshore bottom along transect *P* exhibited higher DIP concentrations and lower N/P ratios (<10) during summer. Furthermore, Figures 3i and 3j show that DIP concentrations along transect P remained relatively consistent during winter and spring.

SUN ET AL. 4 of 17



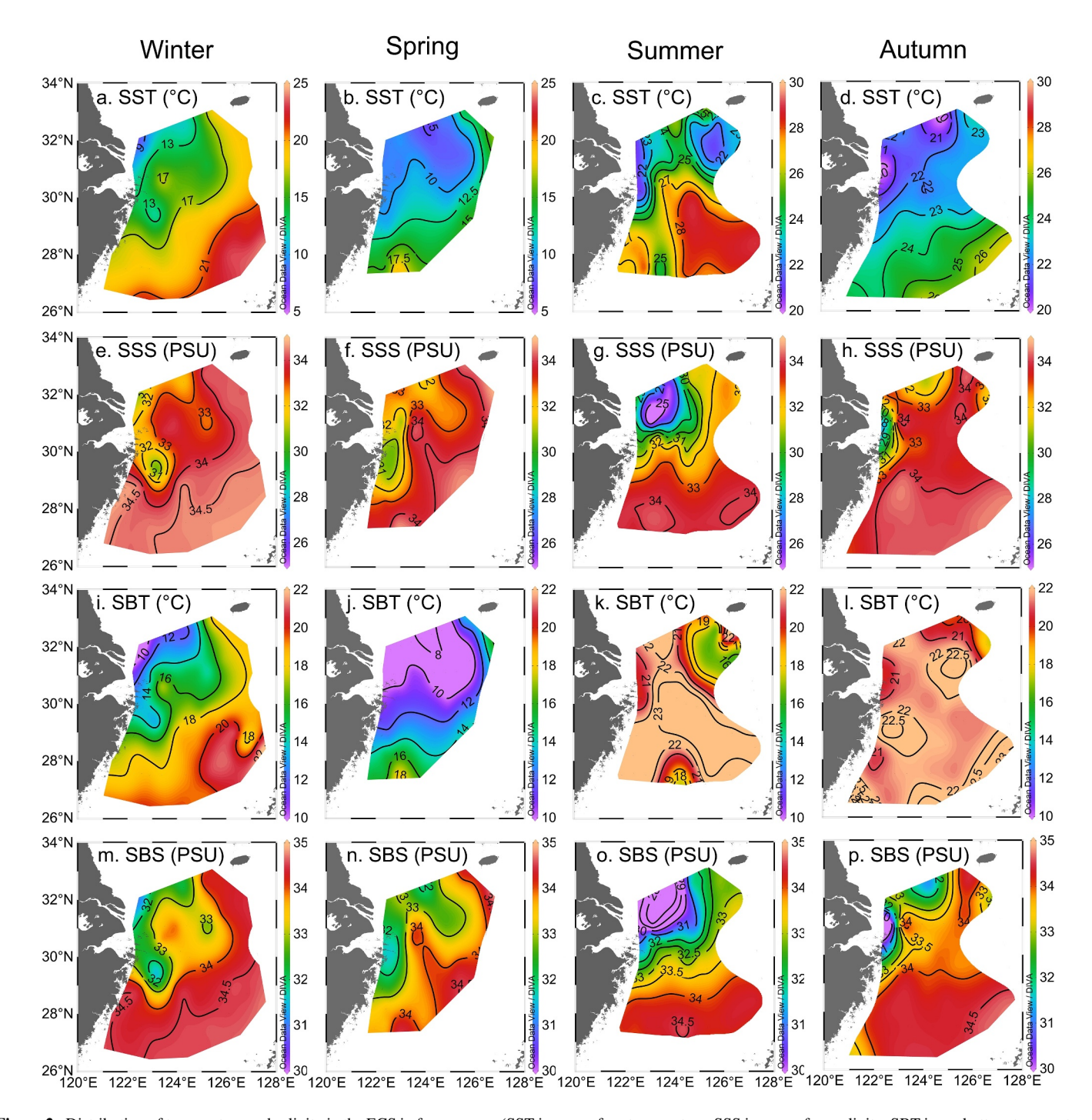


Figure 2. Distribution of temperature and salinity in the ECS in four seasons (SST is sea surface temperature, SSS is sea surface salinity, SBT is sea bottom temperature and SBS is sea bottom salinity).

3.2. Phytoplankton Community Composition and Density

We identified 10 phyla, 163 genera, and 603 species (including varieties, forms, and undetermined species) across all seasons, encompassing diatoms, dinoflagellates, and cyanobacteria. In winter, spring, summer, and autumn, the phytoplankton species number and abundance were 392, 81.19; 303, 160.62; 356, 183.02; and 426, 302.44 cells/mL, respectively. Among these phytoplankton species, the number of diatom species was the highest, followed by dinoflagellate (Table S1 in Supporting Information S1).

SUN ET AL. 5 of 17

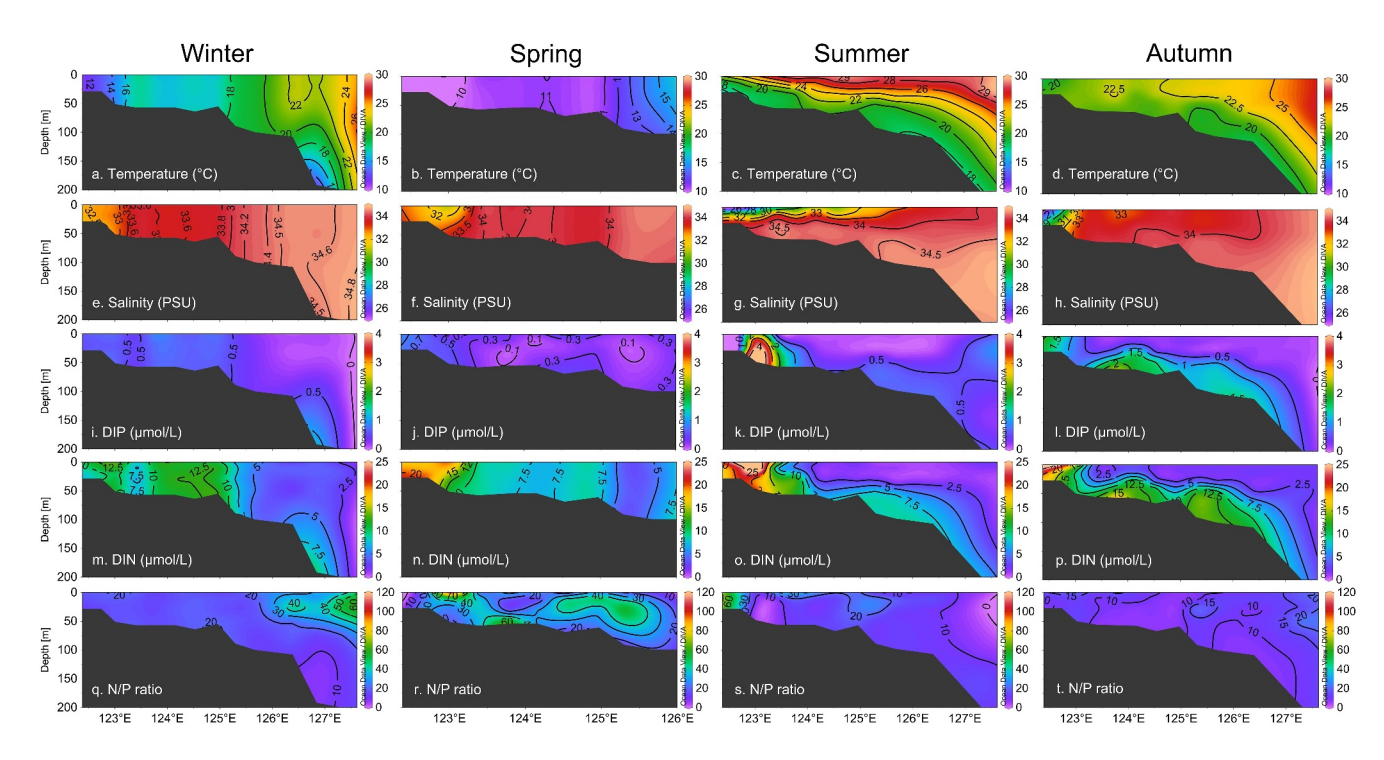


Figure 3. Profiles of temperature, salinity and nutrients (DIN, DIP, N/P) along transect P in all seasons.

According to the results of MDS, cluster analysis, and the spatial variability in hydrological properties, the phytoplankton community of the ECS can be classified as a low-salinity group controlled by coastal currents and CDW, euryhaline groups controlled by shelf mixed water, and oceanic high-temperature and high-salinity groups controlled by Kuroshio (Figure 4). The proportion of classified stations in low-salinity groups was similar in

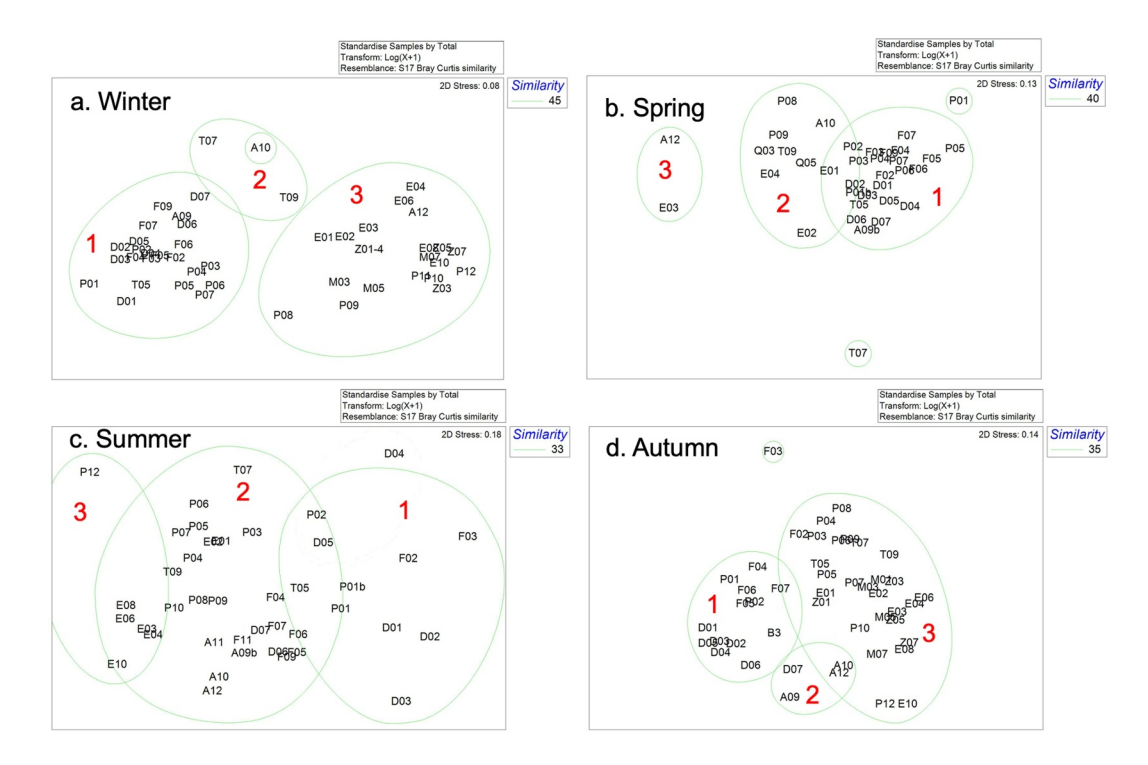


Figure 4. Multidimensional scale analysis and clustering of integrated density of phytoplankton in four seasons (1 = low-salinity groups, 2 = euryhaline groups, 3 = high-salinity groups).

SUN ET AL. 6 of 17



winter (50.0%) and spring (68.6%), mostly contributed by *Paralia sulcata* (No. 10 in Figure 7) and *Thalassiosira pacifica* (No. 3 in Figure 7). The euryhaline groups, such as *Skeletonema* spp (No. 1 in Figure 7) and *Thalassiosira curviseriata* (No. 2 in Figure 7), more widely distributed in summer (58.6%) and spring (25.7%) than that in winter (6.5%) and autumn (6.2%). Moreover, under the intrusion of KSW, the proportion of classified stations in oceanic high-temperature and high-salinity groups in winter (43.5%) and autumn (65.2%) was higher than that in spring (5.7%) and summer (14.6%). The representative species of this group were *Trichodesmium* spp (No. 16 in Figure 7), *Pseudo-nitzschia delicatissima* (No. 5 in Figure 7), *Coccolithus pelagicus* (No. 13 in Figure 7), and *Calcidiscus leptoporus* (No. 19 in Figure 7). The specific location of the three phytoplankton groups was exhibited at Figure S5 in Supporting Information S1.

Along the horizontal scale, DIDs of phytoplankton exhibited significant seasonal variations (Figures S2a–S2d in Supporting Information S1). In winter, DIDs $(1.74 \times 10^7 \text{ cells/m}^2)$ were notably lower compared to other seasons (spring: $4.24 \times 10^7 \text{ cells/m}^2$, summer: $3.84 \times 10^7 \text{ cells/m}^2$, autumn: $6.69 \times 10^7 \text{ cells/m}^2$). In spring, the highest DIDs of phytoplankton were observed in the upwelling area near the Zhoushan Islands, while the highest DIDs of phytoplankton were observed around the front of CDW and Kuroshio in summer and autumn. The DIDs of phytoplankton in the ECS were mostly determined by diatoms and dinoflagellates. The distribution of surface chlorophyll *a* concentration was similar to the distribution of DIDs, with the highest DIDs recorded at station F03 $(92.08 \times 10^7 \text{ cells/m}^2)$ in autumn, while the maximum surface chlorophyll *a* concentration was observed at station D04 (13.39 mg/m^3) in summer (Figure S2 in Supporting Information S1).

Vertically, high phytoplankton abundance was observed on the bottom in spring and on the surface and subsurface layers in summer and autumn. The distribution of diatom abundance was similar to phytoplankton abundance in spring and summer. Notably, dinoflagellate abundance was significantly higher in summer compared to other seasons. Additionally, diatoms and dinoflagellates occupied distinct ecological niches, with diatoms prevalent in the eutrophic nearshore surface and bottom layers, while dinoflagellates were predominantly distributed in the subsurface layer (Figure S3 in Supporting Information S1).

Figure 5 shows that the average abundance of phytoplankton was the highest in the coastal region during winter (24.75 cells/mL), spring (50.44 cells/mL), and summer (66.05 cells/mL), and the highest in the mixed region during autumn (95.82 cells/mL). Notably, the intrusion of the Kuroshio, carrying numerous oceanic dinoflagellate species, resulted in significantly higher relative abundances of dinoflagellates in the coastal region (19.6%), mixed region (32.5%), and Kuroshio region (35.8%) during summer compared to other seasons. Besides, under the intrusion of high temperature and oligotrophic KSW in winter, the abundance of haptophytes in the Kuroshio region exceeded 5.9 cells/mL, with a relative abundance reaching 47.6%.

3.3. Dominant Phytoplankton Species

Figure 6 shows that the dominant species in the ECS mainly consisted of diatoms and dinoflagellates. The diatom *P. sulcata* dominated during winter and spring, with abundances of 21.40 and 57.05 cells/mL, respectively, while *Skeletonema* spp. and *Pseudo-nitzschia pungens* (No. 20 in Figure 7) dominated during summer and autumn, with abundances of 20.84 and 78.65 cells/mL, respectively. Additionally, the abundance of the high-temperature and high-salinity species *Trichodesmium* spp. was higher in autumn compared to other seasons.

3.4. Warm-Water Species and Diversity of Phytoplankton

The distribution of phytoplankton abundance and community structure in the ECS showed obvious regional and seasonal differences. Table 1 and Table S2 in Supporting Information S1 reveal significant differences (p < 0.05) in phytoplankton abundance, warm-water species number, and Shannon index across spatial scales in all seasons. The species number, warm-water species number, and Shannon index were the highest in autumn, followed by winter, summer, and spring. Warm-water species number significantly (p < 0.05) differed in Kuroshio region, mixed region, and coastal region. Furthermore, species number and Shannon index values in the Kuroshio region were significantly higher than that in the coastal and mixed regions.

3.5. Relationship Between Phytoplankton Community and Water Masses

RDA showed significantly (p < 0.01) higher scores for the first axis and for all canonical axes in all seasons, indicating that the ordination results were reliable, and the selected environmental variables explained 74.4%,

SUN ET AL. 7 of 17

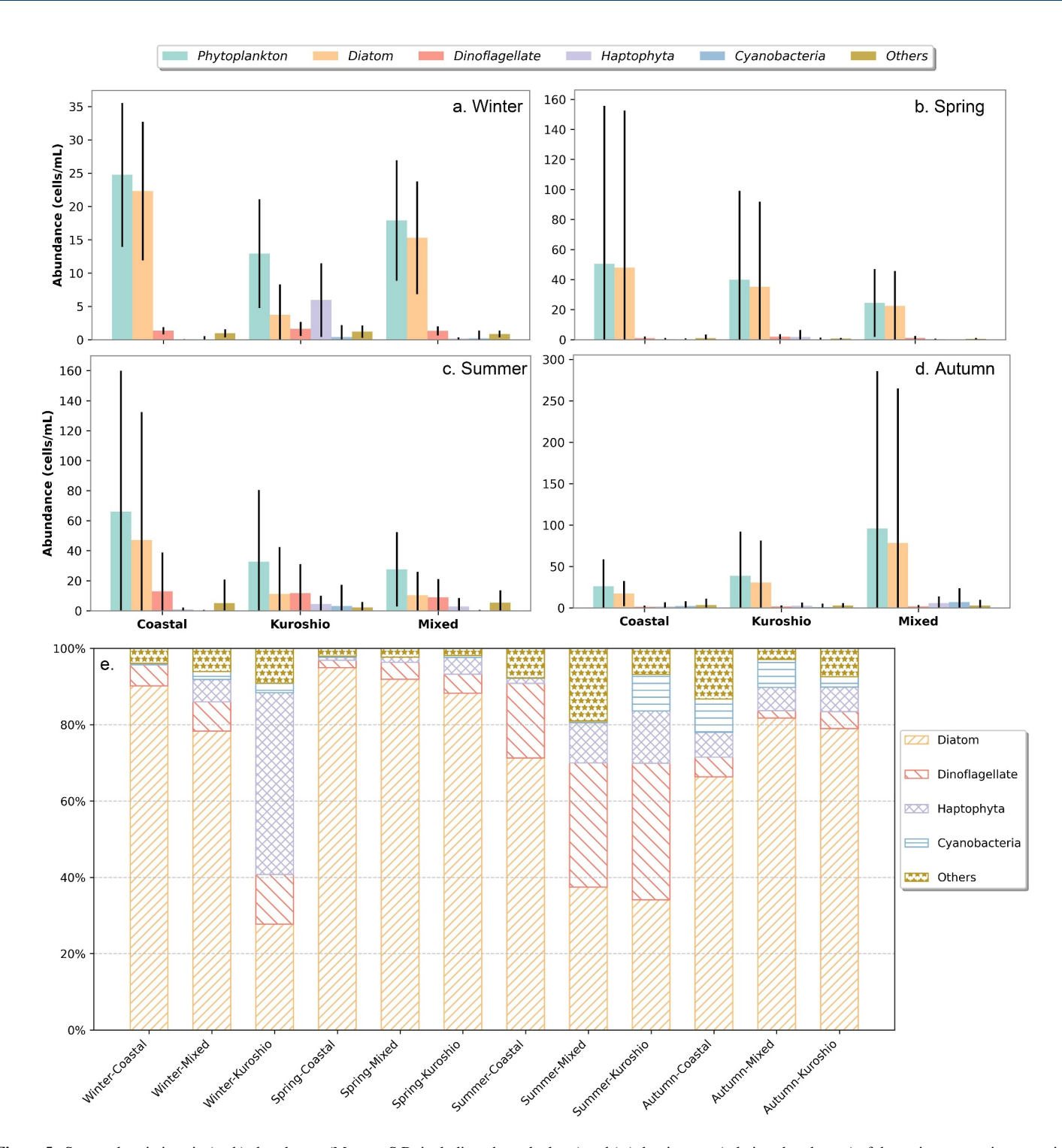


Figure 5. Seasonal variations in (a-d.) abundances (Mean \pm S.D. including phytoplankton) and (e.) dominances (relative abundances) of the main taxonomic groups in all seasons in the ECS.

56.0%, 47.6% and 42.2% of the variation in phytoplankton community composition in winter, spring, summer and autumn, respectively. Temperature accounted for the highest explanation percentages in winter (59.0%) and spring (28.1%), while dissolved inorganic nitrogen (DIN) and turbidity explained the highest percentages in summer (17.9%) and autumn (12.1%), respectively (Figure 7). In winter, the low-salinity species *P. sulcata* (No. 10 in Figure 7) exhibited a positive correlation with nutrients, while oceanic species *C. pelagicus* (No. 13 in

SUN ET AL. 8 of 17

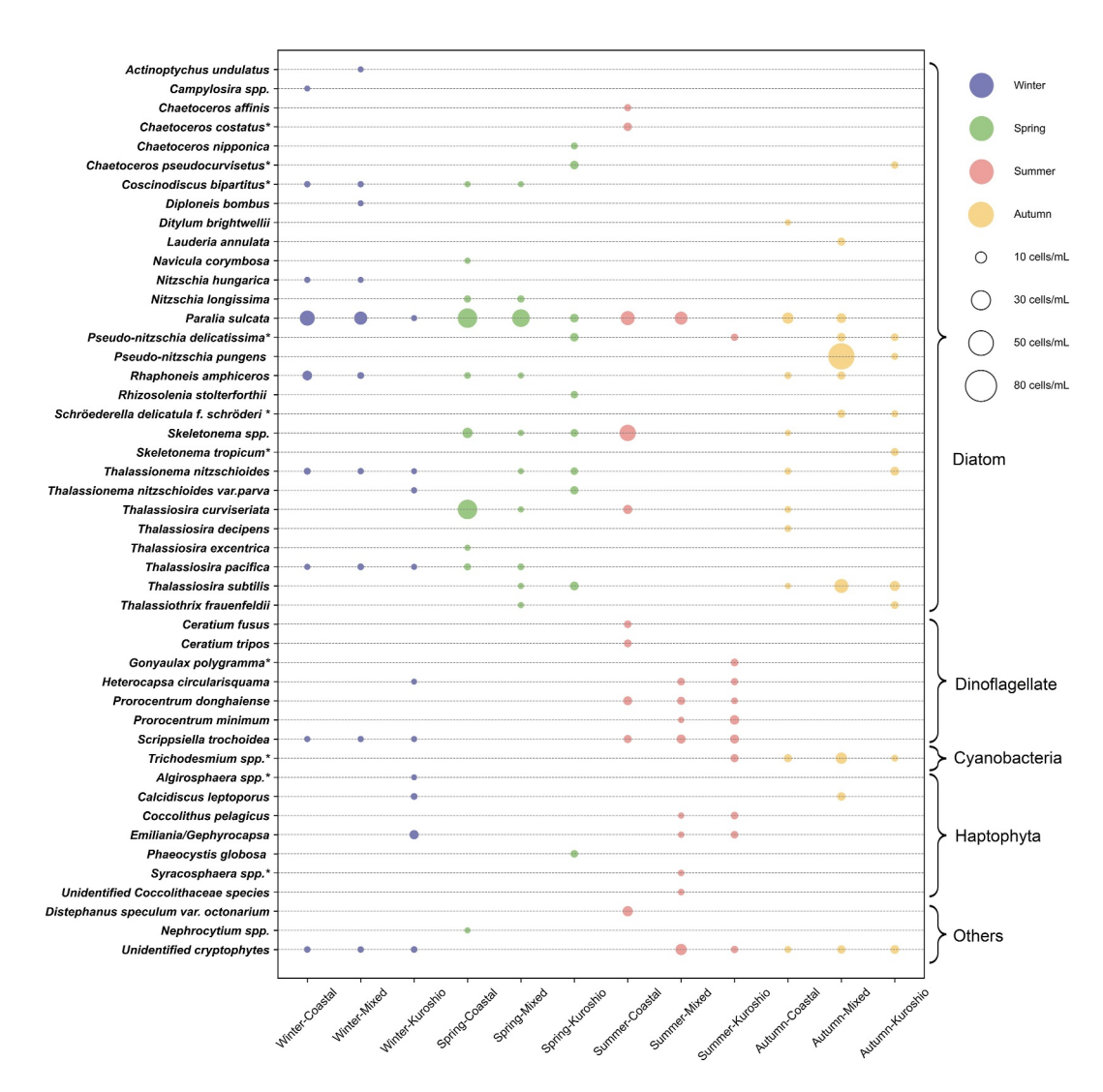


Figure 6. Dominant species and abundance of phytoplankton in different regions in all seasons (* warm-water species).

Figure 7) and *C. leptoporus* (No. 19 in Figure 7) exhibited a positive correlation with depth, temperature and salinity (Figure 7a). In spring, typical warm-water species *P. delicatissima* (No. 5 in Figure 7), *Thalassionema nitzschioides* var. *parva* (No. 6 in Figure 7), and *Chaetoceros pseudocurvisetus* (No. 9 in Figure 7) showed a positive correlation with depth and temperature (Figure 7b). In summer, low-salinity species *P. sulcata* exhibited a positive correlation with nutrients and stratification index, and oceanic species *C. pelagicus* and *Trichodesmium* spp (No. 16 in Figure 7) had a positive correlation with temperature and salinity (Figure 7c). In autumn, *P. sulcata* had a positive correlation with nutrients, while Unidentified *cryptophytes* (No. 12 in Figure 7) showed a positive correlation with salinity (Figure 7d).

In winter, the abundance of phytoplankton and diatoms were significantly (p < 0.05) positively correlated with nutrients and negatively correlated with temperature and salinity. Conversely, chlorophyll a concentration displayed significant (p < 0.05) negative correlations with temperature and salinity. In spring and autumn, all biotic factors were weakly correlated with environmental factors, except the chlorophyll a concentration in spring was significantly (p < 0.05) positively correlated with temperature and salinity. During summer, the correlation patterns between phytoplankton abundance, diatom abundance, and environmental factors resembled those in winter, with the exception of Si/N ratio, which showed an opposite correlation compared to winter (Figure 8).

Figure 9 depicts the modeling results of GAMs with the least Akaike Information Criterion values and the greatest adjusted R^2 and cumulative explained deviation. The spatial variation in phytoplankton abundance and

SUN ET AL. 9 of 17



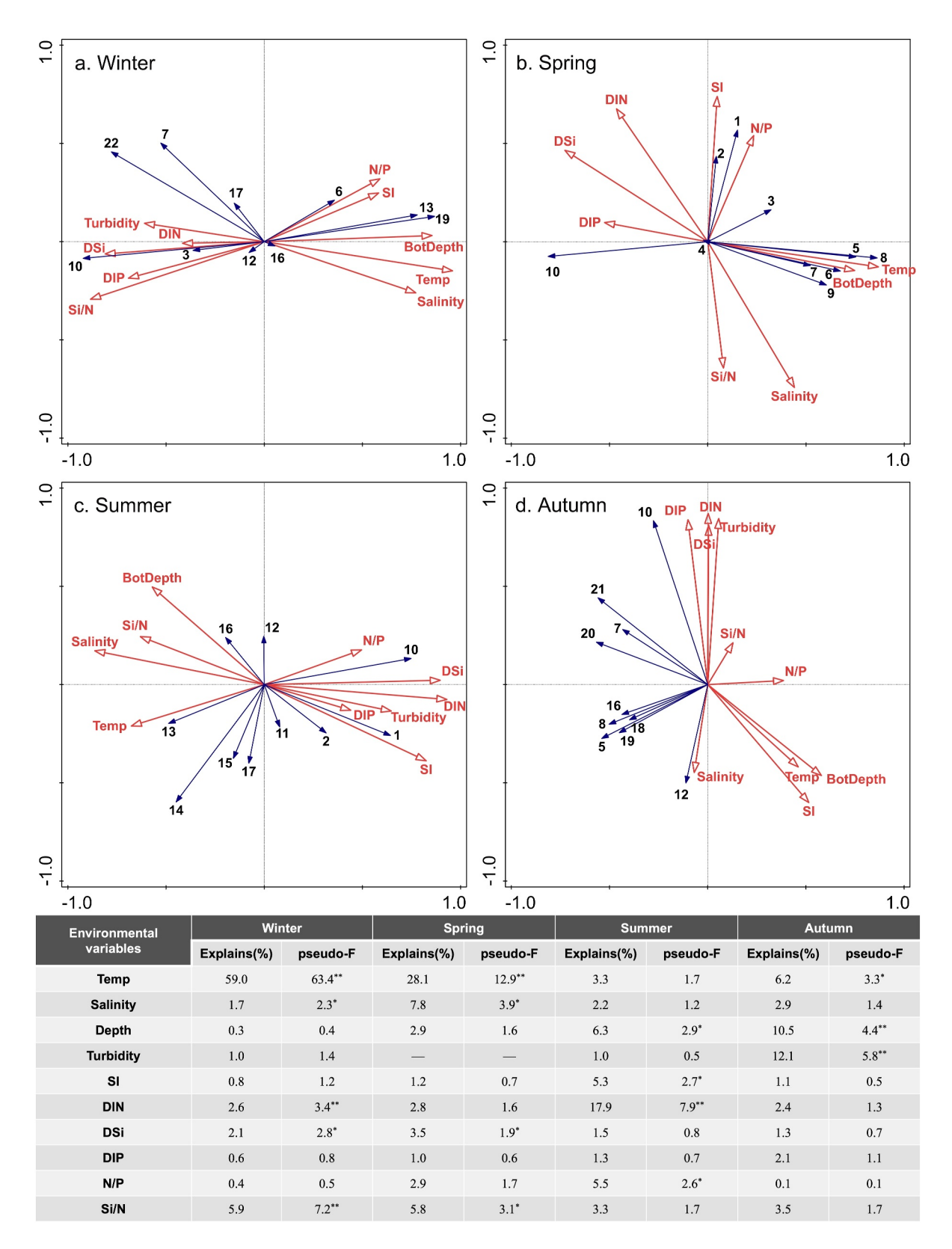


Figure 7.

SUN ET AL. 10 of 17



Table 1Average Values (Mean ± SD) of Species Number, Warm-Water Species Number and Shannon Index in All Seasons

	Winter $(n = 45)$	Spring $(n = 34)$	Summer $(n = 40)$	Autumn ($n = 46$)	Kuroshio ($n = 40$)	Mixed (n = 91)	Coastal $(n = 36)$
Species number	35.1 ± 10.7^{b}	25.2 ± 15.5^{a}	28.4 ± 12.4^{a}	$47.0 \pm 16.6^{\circ}$	84.6 ± 26.9^{a}	70.2 ± 28.4^{b}	59.7 ± 12.9^{b}
Warm-water species number	$14.9 \pm 9.6^{\circ}$	9.6 ± 8.1^{b}	13.6 ± 8.2^{a}	30.9 ± 15.5^{a}	26.4 ± 13.3^{a}	14.9 ± 13.3^{b}	$8.3 \pm 3.5^{\circ}$
Shannon index	2.7 ± 0.5^{b}	2.0 ± 0.7^{a}	2.3 ± 0.6^{a}	2.9 ± 0.7^{c}	3.1 ± 0.5^{a}	2.3 ± 0.6^{b}	2.1 ± 0.6^{b}

Note. A different letter superscript on each line indicates a significant difference.

chlorophyll a concentration were largely explained by physical variables such as salinity, depth, and stratification in all seasons except autumn. In autumn, the spatial variation in phytoplankton abundance (38.2%) and chlorophyll a concentration (31.9%) was mostly explained by turbidity. In the coastal region, the variation in phytoplankton abundance (69.4%) was largely explained by N/P ratio, whereas the variation in chlorophyll a concentration (72.3%) was largely explained by Si/N ratio. In the mixed region, the variation in phytoplankton abundance and chlorophyll a concentration were significantly (p < 0.05) explained by temperature, DSi, Si/N ratio, and stratification. In the Kuroshio region, despite the explanation being low, the variation in phytoplankton abundance (45.3%) was largely explained by the DIP and N/P ratio.

The average N/P ratio of ECS in winter, spring, summer and autumn were 16.3, 28.3, 318.4, and 11.9, respectively. Figure 10 shows that the growth of phytoplankton in the ECS during spring and summer was largely limited by phosphorus, despite the high values of N/P ratio in summer, the limitation was alleviated compared to spring. The growth of phytoplankton in autumn was limited by nitrogen, but the growth of the phytoplankton in winter was not limited by nutrients.

4. Discussion

4.1. Phosphorus Stimulation of Phytoplankton Biomass and Abundance by Kuroshio Intrusion

Phosphate carried by Kuroshio intrusion alleviated the coastal phosphorus limitation in summer, and stimulated the growth of phytoplankton in spring and autumn. As a western boundary current of the Pacific Ocean, the Kuroshio obstructs the direct water exchange between the ECS and the Pacific Ocean. Nevertheless the Kuroshio intrusion can transport nutrients, especially phosphate, from the open ocean into the ECS, resulting in a high correlation between the seasonal changes in KSW and KSSW and the formation of algal blooms in the ECS (Yang et al., 2018). Among the phytoplankton assemblages observed during the four cruises in 2011, a high biomass and abundance of phytoplankton was distributed in the front between the CDW and NKBC in summer and autumn (Figures S2c, S2d, S2g and S2h in Supporting Information S1), as well as in the coastal waters of Zhejiang Province in spring where the KSSW upwelled, generally in accordance with relatively high salinity (Figures S2b and S2f in Supporting Information S1). However, influenced by the low light intensity and low temperature, the phytoplankton biomass and abundance in winter was the minimum. Previous studies focused on single season, indicating that the KSSW intruded onto the ECS shelf with a large number of nutrients (Chen & Wang, 1999; Liu et al., 2003), especially phosphate (Fang, 2004; Yang et al., 2013), and mitigated the nearshore phosphorus limitation and causing algal blooms (Che et al., 2022; Jiang et al., 2015; Xu et al., 2020). The variation in phytoplankton abundance was consistent with the seasonal fluctuation of KSSW intrusion in the ECS. With the increasing KSSW from spring to summer, the area of high phytoplankton biomass and abundance moved northward (Figures S2b, S2c, S2f and S2g in Supporting Information S1). Figure 10 shows most of the sampling stations were limited by phosphorus in spring, although the average N/P ratio in summer was as high as 318.4 due to the massive input of DIN from CDW, with the DIP supplemented by KSSW intrusion, the N/P ratio of certain sampling stations was slightly decreased or equal to 16:1 under the DIP supplemented by KSSW intrusion.

Figure 7. Redundancy analysis ordination of dominant species with environmental variables (upper 30 m) in the ECS in four seasons. 1, Skeletonema spp.; 2, Thalassiosira curviseriata; 3, Thalassiosira pacifica; 4, Nitzschia longissima; 5, Pseudo-nitzschia delicatissima; 6, Thalassionema nitzschioides var. parva; 7, Thalassionema nitzschioides; 8, Thalassiosira subtilis; 9, Chaetoceros pseudocurvisetus; 10, Paralia sulcata; 11, Prorocentrum donghaiense; 12, Unidentified cryptophytes; 13, Coccolithus pelagicus; 14, Prorocentrum minimum; 15, Heterocapsa circularisquama; 16, Trichodesmium spp.; 17, Scrippsiella trochoidea; 18, Schröderella delicatula f. schröderi; 19, Calcidiscus leptoporus; 20, Pseudo-nitzschia pungens; 21, Thalassiosira decipiens; 22, Rhaphoneis amphiceros; Temp, temperature; SI, stratification index; *p < 0.05, **p < 0.01.

SUN ET AL. 11 of 17

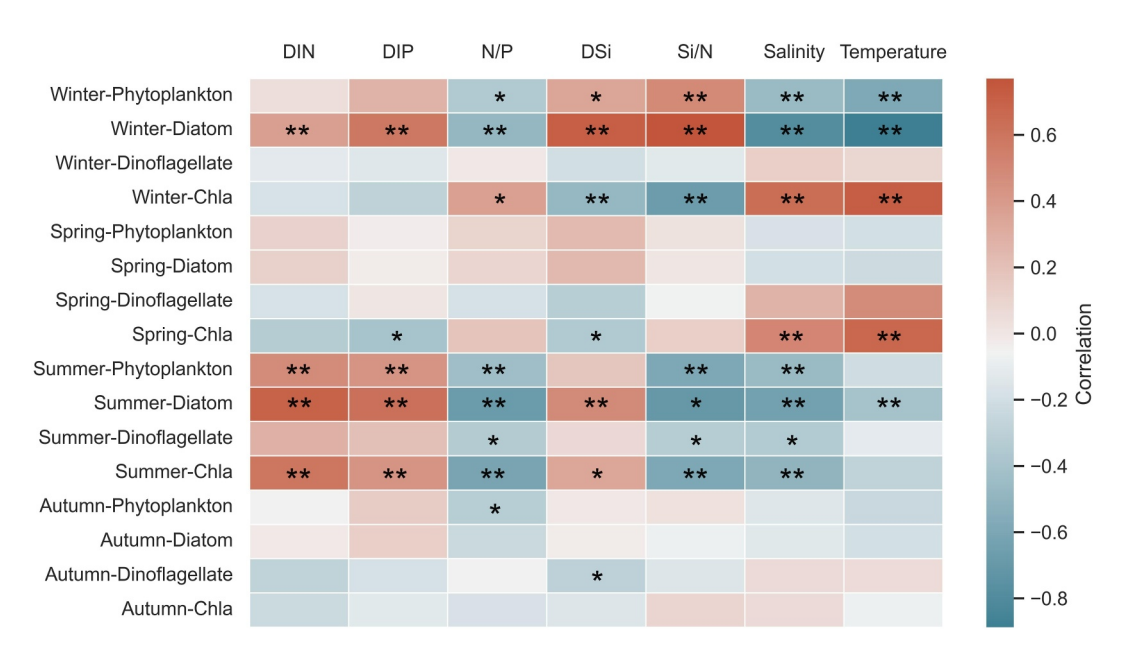


Figure 8. Spearman's rank correlation coefficients between phytoplankton, diatoms, dinoflagellates abundance and chlorophyll *a* concentration and environmental variables (upper 30 m) in all seasons, Chla: chlorophyll *a* concentration.

Besides, due to the severe stratification in summer, and DIP carried by KSSW was transported from the deeper water column, resulting in a large part of DIP remaining in the lower water. In autumn, along with the weakness of stratification and the enhancement of northeast monsoon in autumn, the DIP in the lower water column upwelled and fueled phytoplankton bloom, resulting in higher abundance of phytoplankton in autumn than in other seasons.

The community structure of phytoplankton and distribution of diatoms and dinoflagellates were influenced by the phosphate carried by the Kuroshio. The profiles of temperature, salinity and DIP concentration along transect P in summer indicated KSSW intrusion onto the ECS shelf (Figure 3). Phosphate transported by KSSW supported the growth of diatoms and dinoflagellates, but they occupied different ecological niches due to their disparate nutrient uptake strategies (Zhou et al., 2019). In summer, high diatom abundances were observed on the surface near the shore, while high dinoflagellate abundances were observed in the subsurface water off the shore affected by nutrient concentrations and light availability (Figures S3g and S3k in Supporting Information S1). Previous

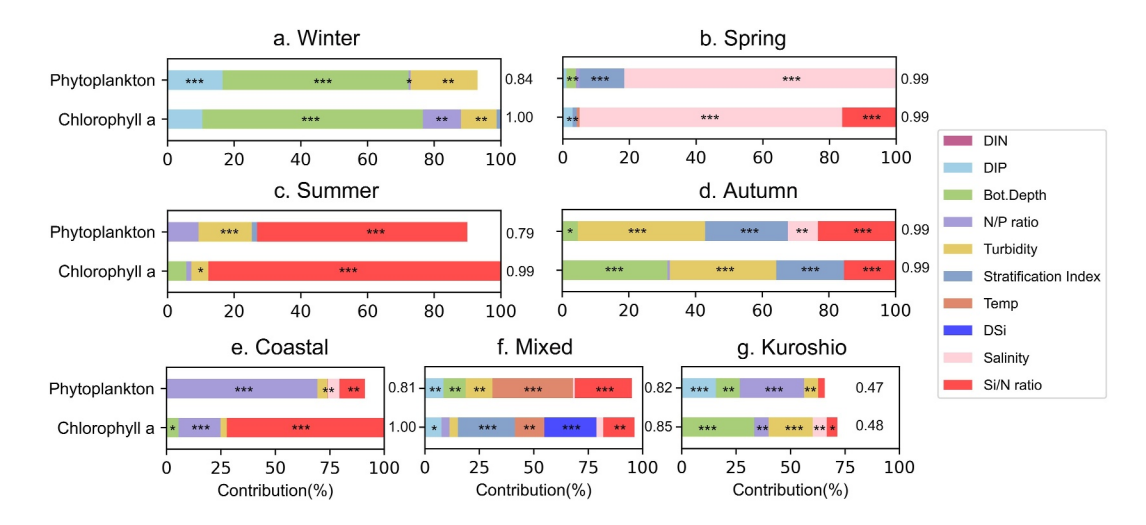


Figure 9. Contribution (cumulative explained deviation) of environmental variables (upper 30 m) to variation in phytoplankton abundance and chlorophyll a concentration in all seasons and three regions (coastal, mixed and Kuroshio) using generalized additive models. Arabic numerals on the right of pillars indicate adjusted R^2 . The asterisks above the pillars indicate significance; *p < 0.05; *p < 0.01; *p < 0.01.

SUN ET AL. 12 of 17

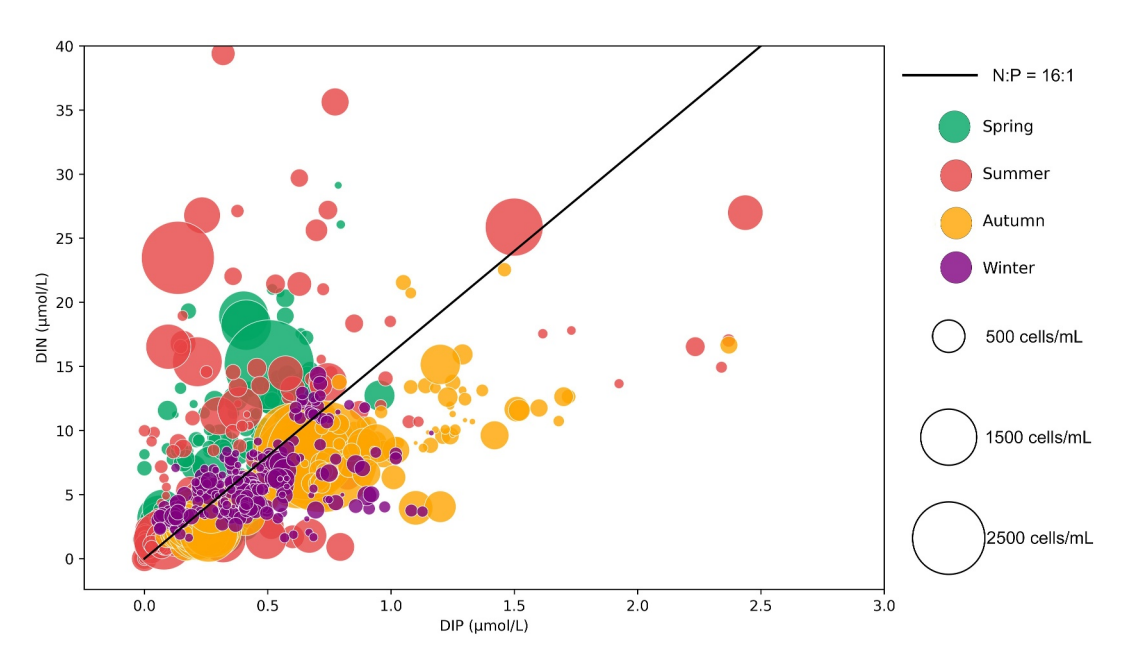


Figure 10. Distribution of phytoplankton abundance along with DIN and DIP in the ECS in all seasons.

studies showed that diatom blooms mainly occurred in nearshore surface water with lower temperature, sufficient light, and abundant nutrients, while dinoflagellate blooms usually occurred in warmer subsurface water (basically >10 m) with relatively scarce nutrients and weak light (Irwin et al., 2012; Lim et al., 2019; Zhang et al., 2019; Zhou et al., 2021). Table S2 in Supporting Information S1 showed the abundance of phytoplankton, diatom, and dinoflagellate was significantly different among seasons and regions. These results indicate that the temporal and spatial distribution of phytoplankton in the ECS was influenced by seasonal changes of circulation, especially the Kuroshio. Figure S4 in Supporting Information S1 shows that there was a well coupling between the surface phytoplankton abundance and the phosphate concentration on the surface and in the 30 m layer, and the GAMs confirmed that DIP and N/P ratio were the main factors affecting phytoplankton abundance and biomass in the coastal and Kuroshio regions (Figures 9e and 9j). These results suggest that the phytoplankton abundance and biomass in the coastal and Kuroshio regions are stimulated by the DIP carried by KSSW.

4.2. Regulation of Phytoplankton Group Composition by Kuroshio Intrusion

According to the results of MDS and cluster analysis, the phytoplankton community of the ECS can be classified as a low-salinity group (mostly diatoms), euryhaline groups, and oceanic high-temperature, high-salinity groups. The representative species were *P. sulcata*, *Skeletonema* spp., and *Trichodesmium* spp., respectively. From the perspective of phytoplankton community species composition, the number of diatom species dominated both the total species number (66.6%) and the dominant species number (65%), because the KSSW intruded onto the ECS shelf and mitigated the nearshore phosphorus limitation. Wu et al. (2016) showed that spatiotemporal patterns of biomarkers reveal higher ratios of diatom/dinoflagellate and diatom/haptophyte in higher productivity areas (CE in summer). Previous studies showed that diatoms have a higher growth rate due to a higher DIN assimilation rate under high turbidity and nutrient concentrations (Goldman & McGillicuddy, 2003; Smayda, 1997). Irwin et al. (2006) found that large phytoplankton cells such as diatoms dominate in eutrophic conditions. Liu et al. (2016) showed that dinoflagellates tend to grow in a lower N/P ratio environment rather than diatoms. Diatoms and dinoflagellates were dominant in the coastal and mixed regions, while cyanobacteria and small-celled phytoplankton were dominant in the oligotrophic Kuroshio region (Figure 5).

Affected by the KSW intrusion, the haptophytes including *Emiliania huxleyi/Gephyrocapsa oceanica* and *C. pelagicus* were the absolutely dominant species in the Kuroshio region in winter, accounting for 47.6% of the relative abundance. In spring, algal blooms occurred in KSSW upwelling areas, and the phytoplankton ecological types are mainly nearshore low-salinity species and eurytherm euryhaline species (Figure 6), among which *P. sulcata* (35.5%) and *Thalassiosira curviseriata* (18.1%, No. 2 in Figure 7) occupied a high proportion. In summer,

SUN ET AL. 13 of 17



the CDW carried low salinity water with sufficient nutrients, especially DIN and DSi, into the ECS, and the upwelling of KSSW provided abundant phosphate, which was conducive to the growth of large-celled diatoms and low-salinity phytoplankton species. The intrusion of KSSW in summer was an important mechanism for phosphate replenishment in the CE and Zhejiang Province coastal waters (Tseng et al., 2014; Wang et al., 2016; L. Xu et al., 2018; Yang et al., 2013) and affected the phytoplankton community composition in the ECS during summer (Jiang, Chen, Zhai, et al., 2019; Noman et al., 2019; Xu et al., 2020; Q. Xu et al., 2019, Y. Xu et al., 2019). In autumn, diatoms (particularly *P. pungens*) bloomed in the mixed region between the coastal low-salinity waters and Kuroshio affected waters where DIP limitation was reduced (Figure 10). Moreover, the distribution of the high-salinity groups in winter and autumn was consistent with the range of the KSW intruding the ECS, whereas the KSSW intruded the ECS from bottom in spring and summer, resulting in the few distribution of hightemperature and high-salinity groups (Figure S5 in Supporting Information S1). RDA results show that the phytoplankton low-salinity species were regulated by coastal currents with rich nutrients and warm-water species were regulated by Kuroshio with high temperature and high salinity (Figure 7). Our studies demonstrated that the Kuroshio carried abundant phosphates and high-temperature, high-salinity water mass intruded into the ECS, which profoundly affected the phytoplankton community composition in the ECS and caused significant spatial differences.

4.3. Enhancement of Phytoplankton Diversity by Kuroshio Intrusion

The phosphates carried by Kuroshio intrusion will not only affect the abundance distribution and group composition of phytoplankton, but also decrease phytoplankton diversity (species number, warm-water species number, and Shannon index) in the coastal region and increase phytoplankton diversity in the Kuroshio region across all seasons (Table 1 and Figure S1 in Supporting Information S1). KSSW transferred abundant phosphate to the ECS coastal region that mitigated the nearshore phosphorus limit, promoted the blooms of low-salinity diatoms, and occupied the ecological niches of other groups, leading to a low phytoplankton diversity in the coastal region. Previous studies have found that HABs reduced phytoplankton community diversity (Amorim & Moura, 2021; Chai et al., 2020). Furthermore, temperature was another main driver affecting phytoplankton species diversity (Benedetti et al., 2021; Ibarbalz et al., 2019; Righetti et al., 2019). High temperatures promoted phytoplankton species diversity by enhancing speciation, increasing metabolic rates and so on (Beaugrand et al., 2013; Tittensor et al., 2010). Therefore, the high temperature water carried by the KSW was conducive to increasing the phytoplankton species diversity in the Kuroshio region. Table 1 shows that the intrusion of KSW resulted in significantly higher species number and Shannon diversity index of phytoplankton in winter and autumn compared to spring and summer. Besides, the species number and Shannon diversity index in the Kuroshio region were significantly higher than those in the coastal and mixed regions.

The Kuroshio intrusion also carried a large number of warm-water species, which had an important impact on phytoplankton diversity over the ECS. Table 1 and Table S2 in Supporting Information S1 show that the warm-water species number in the Kuroshio region were significantly higher than that in the coastal and mixed regions across all seasons. Jiang et al. (2015) showed that the tropical/subtropical warm-water and high-salinity species carried by Kuroshio influenced the phytoplankton community composition and species diversity of the CE. *Trichodesmium* spp. was the indicator species of Kuroshio intrusion (Jiang et al., 2018, 2023), and phytoplankton mainly consisted of high-temperature and high-salinity species and warm-water species (Wang et al., 2020). The circulation changes of Kuroshio, TWC and CDW and the fluctuation of water masses had important effects on the composition and distribution of phytoplankton communities in the CE and the adjacent ECS shelf (Jiang et al., 2014, 2015, 2019). Therefore, we demonstrated that the Kuroshio, as a "seed bank" of phytoplankton warmwater species, carried a large number of tropical/subtropical species and heat to the ECS and enhanced the phytoplankton diversity in the ECS.

5. Conclusions

Four cruises were conducted in the ECS across four seasons of 2011 to explore the potential influence of Kuroshio intrusion on the phytoplankton community. The phytoplankton species mainly consisted of diatoms and dinoflagellates, and high biomass of phytoplankton was observed in the coastal region where the KSSW intruded and upwelled. The phytoplankton biomass, community composition, and diversity significantly differed from temporally to spatially, and were tightly coupled with the changes in KSW and KSSW. The phosphate carried by the Kuroshio intrusion promoted the growth of phytoplankton and affected the distribution of phytoplankton

SUN ET AL. 14 of 17



biomass and community composition. Moreover, the warm-water species and heat transported by the Kuroshio enhanced the phytoplankton diversity in the ECS. Nevertheless, it is worth noting that the survey stations across the four seasons in this study were not uniformly distributed. This variability may impact the comparison of survey results across different temporal and spatial scales. Additionally, the microscopic examination cannot identify pico-phytoplankton, further studies need to be performed on phytoplankton community composition using molecular sequencing.

List of Acronyms

CDW Changjiang Diluted Water

CE Changjiang Estuary

DIDs Depth-integrated densities

DIN Dissolved inorganic nitrogen

DIP Dissolved inorganic phosphorus

ECS East China Sea

GAMs Generalized additive models

KSSW Kuroshio Subsurface Water

KSW Kuroshio Surface Water

MDS Multidimensional scaling

NKBC Nearshore Kuroshio Branch Current

RDA Redundancy analysis

TWC Taiwan Warm Current

Data Availability Statement

Data set of phytoplankton abundance for this paper are freely available online through Figshare (http://dx.doi.org/10.6084/m9.figshare.25833949). The temperature, salinity, nutrient, and chlorophyll *a* data sets are attributed to Jiang et al. (2018). Figures were made with the software blow: PRIMER (Clarke & Gorley, 2006) is available under the license at https://www.primer-e.com/software. Canoco five is available under the license at http://www.canoco5.com. Ocean Data View version 5.6.2 (Schlitzer, 2018) is available at http://odv.awi.de. *R* software version 4.4.1 (R Core Team, 2024) is available at https://www.R-project.org.

Acknowledgments We are grateful to Prof. Wensheng Jiang

for providing the data of temperature,

salinity, and turbidity. This work was

Science Foundation of China

funded by the Zhejiang Provincial Natural

(LR22D060001), National Natural Science

Foundation of China (41876198), Project

of State Key Laboratory of Satellite Ocean

Environment Dynamics, Second Institute

National Basic Research Program of China

term Observation and Research Plan in the

(2010CB428903), and Project of Long-

Changjiang Estuary and Adjacent East

China Sea (LORCE; SZ2001).

of Oceanography (SOEDZZ2202),

Amorim, C. A., & Moura, A. D. N. (2021). Ecological impacts of freshwater algal blooms on water quality, plankton biodiversity, structure, and ecosystem functioning. *Science of the Total Environment*, 758, 143605. https://doi.org/10.1016/j.scitotenv.2020.143605

Beaugrand, G., Rombouts, I., & Kirby, R. R. (2013). Towards an understanding of the pattern of biodiversity in the oceans. *Global Ecology and Biogeography*, 22(4), 440–449. https://doi.org/10.1111/geb.12009

Benedetti, F., Vogt, M., Elizondo, U. H., Righetti, D., Zimmermann, N. E., & Gruber, N. (2021). Major restructuring of marine plankton assemblages under global warming. *Nature Communications*, 12(1), 5226. https://doi.org/10.1038/s41467-021-25385-x

Bian, C., Jiang, W., & Greatbatch, R. J. (2013). An exploratory model study of sediment transport sources and deposits in the Bohai Sea, Yellow Sea, and East China Sea. *Journal of Geophysical Research: Oceans*, 118(11), 5908–5923. https://doi.org/10.1002/2013JC009116

Chai, Z. Y., Wang, H., Deng, Y., Hu, Z., & Zhong Tang, Y. (2020). Harmful algal blooms significantly reduce the resource use efficiency in a coastal plankton community. Science of the Total Environment, 704, 135381. https://doi.org/10.1016/j.scitotenv.2019.135381

Che, H., Zhang, J., Liu, Q., & Zhao, M. (2022). A driving factor for harmful algal blooms in the East China Sea coastal marine ecosystems — Implications of Kuroshio subsurface water invasion. *Marine Pollution Bulletin*, 181, 113871. https://doi.org/10.1016/j.marpolbul.2022.113871 Chen, C. T. A. (2009). Chemical and physical fronts in the Bohai, Yellow and East China seas. *Journal of Marine Systems*, 78(3), 394–410. https://doi.org/10.1016/j.jmarsys.2008.11.016

Chen, C. T. A., & Wang, S. L. (1999). Carbon, alkalinity and nutrient budgets on the East China Sea continental shelf. *Journal of Geophysical Research*, 104, 20675–20686. https://doi.org/10.1029/1999JC900055

Chen, Y. L. L., Chen, H. Y., Gong, G. C., Lin, Y. H., Jan, S., & Takahashi, M. (2004). Phytoplankton production during a summer coastal upwelling in the East China Sea. Continental Shelf Research, 24(12), 1321–1338. https://doi.org/10.1016/j.csr.2004.04.002

SUN ET AL. 15 of 17



- Clarke, K. R., & Gorley, R. N. (2006). Primer v6: User manual/Tutorial: Plymouth marine laboratory [Software]. https://www.primer-e.com/software
- Fang, T. H. (2004). Phosphorus speciation and budget of the East China sea. Continental Shelf Research, 24(12), 1285–1299. https://doi.org/10.1016/j.csr.2004.04.003
- Goldman, J. C., & McGillicuddy, D. J. J. (2003). Effect of large marine diatoms growing at low light on episodic new production. *Limnology & Oceanography*, 48(3), 1176–1182. https://doi.org/10.4319/lo.2003.48.3.1176
- Gong, G. C., Lee Chen, Y. L., & Liu, K. K. (1996). Chemical hydrography and chlorophyll a distribution in the East China sea in summer: Implications in nutrient dynamics. Continental Shelf Research, 16(12), 1561–1590. https://doi.org/10.1016/0278-4343(96)00005-2
- Guo, S., Feng, Y., Wang, L., Dai, M., Liu, Z., Bai, Y., & Sun, J. (2014). Seasonal variation in the phytoplankton community of a continental-shelf sea: The East China sea. *Marine Ecology Progress Series*, 516(3), 103–126. https://doi.org/10.3354/meps10952
- Harrison, P. J., Hu, M. H., Yang, Y. P., & Lu, X. (1990). Phosphate limitation in estuarine and coastal waters of China. *Journal of Experimental Marine Biology and Ecology*, 140(1), 79–87. https://doi.org/10.1016/0022-0981(90)90083-O
- Ibarbalz, F. M., Henry, N., Brandão, M. C., Martini, S., Busseni, G., Byrne, H., et al. (2019). Global trends in marine plankton diversity across kingdoms of life. *Cell*, 179(5), 1084–1097. https://doi.org/10.1016/j.cell.2019.10.008
- Irwin, A. J., Finkel, Z. V., Schofield, O. M. E., & Falkowski, P. G. (2006). Scaling-up from nutrient physiology to the size-structure of phyto-plankton communities. *Journal of Plankton Research*, 28(5), 459–471. https://doi.org/10.1093/plankt/fbi148
- Irwin, A. J., Nelles, A. M., & Finkel, Z. V. (2012). Phytoplankton niches estimated from field data. Limnology & Oceanography, 57(3), 787–797. https://doi.org/10.4319/lo.2012.57.3.0787
- Jiang, Z., Chen, J., Gao, Y., Zhai, H., Jin, H., Zhou, F., et al. (2019). Regulation of spatial changes in phytoplankton community by water column stability and nutrients in the southern Yellow Sea. *Journal of Geophysical Research: Biogeosciences*, 124(8), 2610–2627. https://doi.org/10. 1029/2018/G004785
- Jiang, Z., Chen, J., Zhai, H., Zhou, F., Yan, X., Zhu, Y., et al. (2019). Kuroshio shape composition and distribution of filamentous diazotrophs in the East China sea and southern Yellow Sea. *Journal of Geophysical Research: Oceans*, 124(11), 7421–7436. https://doi.org/10.1029/20191C015413
- Jiang, Z., Chen, J., Zhou, F., Shou, L., Wang, K., Tao, B., et al. (2015). Controlling factors of summer phytoplankton community in the Changjiang (Yangtze river) estuary and Adjacent East China sea shelf. Continental Shelf Research, 101, 71–84. https://doi.org/10.1016/j.csr.2015.04.009
 Jiang, Z., Li, H., Zhai, H., Zhou, F., Chen, Q., Chen, J., et al. (2018). Seasonal and spatial changes in Trichodesmium associated with physi-
- Jiang, Z., Li, H., Zhai, H., Zhou, F., Chen, Q., Chen, J., et al. (2018). Seasonal and spatial changes in *Trichodesmium* associated with physicochemical properties in east China sea and southern Yellow Sea. *Journal of Geophysical Research: Biogeosciences*, 123(2), 509–530. https://doi.org/10.1002/2017JG004275
- Jiang, Z., Liu, J., Chen, J., Chen, Q., Yan, X., Xuan, J., & Zeng, J. (2014). Responses of summer phytoplankton community to drastic environmental changes in the Changjiang (Yangtze River) estuary during the past 50 years. Water Research, 54, 1–11. https://doi.org/10.1016/j.watres 2014.01.032
- Jiang, Z., Zhu, Y., Sun, Z., Zhai, H., Zhou, F., Yan, X., et al. (2023). Enhancement of summer nitrogen fixation by the Kuroshio intrusion in the East China sea and southern Yellow Sea. *Journal of Geophysical Research: Biogeosciences*, 128(3), e2022JG007287. https://doi.org/10.1029/ 2022JG007287
- Kobayashi, S., & Fujiwara, T. (2008). Long-term variability of shelf water intrusion and its influence on hydrographic and biogeochemical properties of the Seto Inland Sea, Japan. *Journal of Oceanography*, 64(4), 595–603. https://doi.org/10.1007/s10872-008-0050-0
- Kondo, M. (1985). Oceanographic investigations of fishing grounds in the East China Sea and the Yellow Sea i. characteristics of the mean temperature and salinity distributions measured at 50 meters and near the bottom. *Bulletin of the Seikai National Fisheries Research Institute*, 62, 19–66. https://cir.nii.ac.jp/crid/1371132818587463811
- Li, J., Glibert, P., Zhou, M., Lu, S., & Lu, D. (2009). Relationships between nitrogen and phosphorus forms and ratios and the development of dinoflagellate blooms in the East China Sea. *Marine Ecology Progress Series*, 383, 11–26. https://doi.org/10.3354/meps07975
- Lian, E., Yang, S., Wu, H., Yang, C., Li, C., & Liu, J. T. (2016). Kuroshio subsurface water feeds the wintertime Taiwan Warm Current on the inner East China Sea shelf. *Journal of Geophysical Research: Oceans*, 121(7), 4790–4803. https://doi.org/10.1002/2016JC011869
- Lim, A. S., Jeong, H. J., Ok, J. H., You, J. H., Kang, H. C., & Kim, S. J. (2019). Effects of light intensity and temperature on growth and ingestion rates of the mixotrophic dinoflagellate *Alexandrium pohangense*. *Marine Biology*, 166(7), 98. https://doi.org/10.1007/s00227-019-3546-9
- Liu, K. K., Peng, T. H., Shaw, P. T., & Shiah, F. K. (2003). Circulation and biogeochemical processes in the East China sea and the vicinity of Taiwan: An overview and a brief synthesis. *Deep Sea Research Part II: Topical Studies in Oceanography*, 50(6), 1055–1064. https://doi.org/10.1016/S0967-0645(03)00009-2
- Liu, X., Xiao, W., Landry, M. R., Chiang, K. P., Wang, L., & Huang, B. (2016). Responses of phytoplankton communities to environmental variability in the East China Sea. *Ecosystems*, 19(5), 832–849. https://doi.org/10.1007/s10021-016-9970-5
- Noman, M. A., Sun, J., Gang, Q., Guo, C., Islam, M. S., Li, S., & Yue, J. (2019). Factors regulating the phytoplankton and tintinnid micro-zooplankton communities in the East China Sea. *Continental Shelf Research*, 181, 14–24. https://doi.org/10.1016/j.csr.2019.05.007
- Oey, L. Y., Hsin, Y. C., & Wu, C. R. (2010). Why does the Kuroshio northeast of Taiwan shift shelfward in winter? *Ocean Dynamics*, 60(2), 413–426. https://doi.org/10.1007/s10236-009-0259-5
- Qu, H., Xu, Y., Wang, J., & Li, X. Z. (2020). Radiolarian assemblages in the shelf area of the East China Sea and Yellow Sea and their ecological indication of the Kuroshio Current derivative branches. *PeerJ*, 8, e9976. https://doi.org/10.7717/peerj.9976
- Qu, T., Tozuka, T., Kida, S., Guo, X., Miyazawa, Y., & Liu, Q. (2016). Western Pacific and marginal sea processes. In *Indo-pacific climate variability and predictability* (pp. 151–186). World Scientific. https://doi.org/10.1142/9789814696623_0006
- R Core Team. (2024). R: A language and environment for statistical computing [Software]. R Foundation for Statistical Computing. Retrieved from https://www.R-project.org
- Righetti, D., Vogt, M., Gruber, N., Psomas, A., & Zimmermann, N. E. (2019). Global pattern of phytoplankton diversity driven by temperature and environmental variability. Science Advances, 5(5), eaau6253. https://doi.org/10.1126/sciadv.aau6253
- Schlitzer, R. (2018). Ocean data View [Software]. ODV. http://odv.awi.de
- Shannon, C. E. (1948). A mathematical theory of communication. *Bell System Technical Journal*, 27(3), 379–423. https://doi.org/10.1002/j.1538-7305.1948.tb01338.x
- Smayda, T. J. (1997). Harmful algal blooms: Their ecophysiology and general relevance to phytoplankton blooms in the sea. Limnology & Oceanography, 42, 1137–1153. https://doi.org/10.4319/lo.1997.42.5_part_2.1137
- Sun, Z. (2024). Phytoplankton abundance data set of East China Sea in 2011 [Dataset]. xlsx. https://doi.org/10.6084/m9.figshare.25833949.v2 ter Braak, C. J. F., & Smilauer, P. (2012). Canoco reference manual and user's guide: Software for ordination, version 5.0 [Software]. Microcomputer Power. http://www.canoco5.com

SUN ET AL. 16 of 17



- Tittensor, D. P., Mora, C., Jetz, W., Lotze, H. K., Ricard, D., Berghe, E. V., & Worm, B. (2010). Global patterns and predictors of marine biodiversity across taxa. *Nature*, 466(7310), 1098–1101. https://doi.org/10.1038/nature09329
- Trommer, G., Leynaert, A., Klein, C., Naegelen, A., & Beker, B. (2013). Phytoplankton phosphorus limitation in a North Atlantic coastal ecosystem not predicted by nutrient load. *Journal of Plankton Research*, 35(6), 1207–1219. https://doi.org/10.1093/plankt/fbt070
- Tseng, Y. F., Lin, J., Dai, M., & Kao, S. J. I. (2014). Joint effect of freshwater plume and coastal upwelling on phytoplankton growth off the Changjiang River. *Biogeosciences*, 11(2), 409–423. https://doi.org/10.5194/bg-11-409-2014
- Wang, J., Bouwman, A. F., Liu, X., Beusen, A. H. W., Van Dingenen, R., Dentener, F., et al. (2021). Harmful algal blooms in Chinese coastal waters will persist due to perturbed nutrient ratios. *Environmental Science and Technology Letters*, 8(3), 276–284. https://doi.org/10.1021/acs.estlett.1c00012
- Wang, W., Yu, Z., Song, X., Wu, Z., Yuan, Y., Zhou, P., & Cao, X. (2016). The effect of Kuroshio Current on nitrate dynamics in the southern East China Sea revealed by nitrate isotopic composition. *Journal of Geophysical Research: Oceans*, 121(9), 7073–7087. https://doi.org/10.1002/ 2016JC011882
- Wang, W., Yu, Z., Song, X., Yuan, Y., Wu, Z., Zhou, P., & Cao, X. (2018). Intrusion pattern of the offshore Kuroshio branch current and its effects on nutrient contributions in the East China Sea. *Journal of Geophysical Research: Oceans*, 123(3), 2116–2128. https://doi.org/10.1002/2017JC013538
- Wang, X., Wei, Y., Wu, C., Guo, C., & Sun, J. (2020). The profound influence of Kuroshio intrusion on microphytoplankton community in the northeastern South China Sea. Acta Oceanologica Sinica, 39(8), 79–87. https://doi.org/10.1007/s13131-020-1608-y
- Wu, C., Hsin, Y., Chiang, T., Lin, Y. F., & Tsui, I. F. (2014). Seasonal and interannual changes of the Kuroshio intrusion onto the East China Sea. Journal of Geophysical Research: Oceans, 119(8), 5039–5051. https://doi.org/10.1002/2013JC009748
- Wu, P., Bi, R., Duan, S., Jin, H., Chen, J., Hao, Q., et al. (2016). Spatiotemporal variations of phytoplankton in the East China Sea and the Yellow Sea revealed by lipid biomarkers. *Journal of Geophysical Research: Biogeosciences*, 121(1), 109–125. https://doi.org/10.1002/2015JG003167
- Wu, Y., Zhang, Y., & Zhou, C. (2000). Phytoplankton distribution and community structure in the East China Sea (ECS) continental shelf. Chinese Journal of Oceanology and Limnology, 18(1), 74–79. https://doi.org/10.1007/BF02842545
- Xu, L., Yang, D., Benthuysen, J. A., & Yin, B. (2018). Key dynamical factors driving the Kuroshio subsurface water to reach the Zhejiang coastal area. *Journal of Geophysical Research: Oceans*, 123(12), 9061–9081. https://doi.org/10.1029/2018JC014219
- Xu, L., Yang, D., Greenwood, J., Feng, X., Gao, G., Qi, J., et al. (2020). Riverine and oceanic nutrients govern different algal bloom domain near the Changjiang estuary in summer. *Journal of Geophysical Research: Biogeosciences*, 125(10), e2020JG005727. https://doi.org/10.1029/ 2020JG005727
- Xu, Q., Sukigara, C., Goes, J. I., Gomes, H., Zhu, Y., Wang, S., et al. (2019). Interannual changes in summer phytoplankton community composition in relation to water mass variability in the East China Sea. *Journal of Oceanography*, 75(1), 61–79. https://doi.org/10.1007/s10872-018-0484-y
- Xu, Y., Ma, L., Sun, Y., Li, X., Wang, H., & Zhang, H. (2019). Spatial variation of demersal fish diversity and distribution in the East China Sea: Impact of the bottom branches of the Kuroshio Current. *Journal of Sea Research*, 144, 22–32. https://doi.org/10.1016/j.seares.2018.11.003
- Xu, Y., Yu, F., Li, X., Ma, L., Dong, D., Kou, Q., et al. (2018). Spatiotemporal patterns of the macrofaunal community structure in the East China Sea, off the coast of Zhejiang, China, and the impact of the Kuroshio branch current. *PLoS One*, 13(1), e0192023. https://doi.org/10.1371/journal.pone.0192023
- Yang, D., Yin, B., Chai, F., Feng, X., Xue, H., Gao, G., & Yu, F. (2018). The onshore intrusion of Kuroshio subsurface water from February to July and a mechanism for the intrusion variation. *Progress in Oceanography*, 167, 97–115. https://doi.org/10.1016/j.pocean.2018.08.004
- Yang, D., Yin, B., Liu, Z., Bai, T., Qi, J., & Chen, H. (2012). Numerical study on the pattern and origins of Kuroshio branches in the bottom water of southern East China Sea in summer. *Journal of Geophysical Research*, 117, C02014. https://doi.org/10.1029/2011JC007528
- Yang, D., Yin, B., Liu, Z., & Feng, X. (2011). Numerical study of the ocean circulation on the East China Sea shelf and a Kuroshio bottom branch northeast of Taiwan in summer. *Journal of Geophysical Research*, 116, C05015. https://doi.org/10.1029/2010JC006777
- Yang, D., Yin, B., Sun, J., & Zhang, Y. (2013). Numerical study on the origins and the forcing mechanism of the phosphate in upwelling areas off the coast of Zhejiang province, China in summer. *Journal of Marine Systems*, 123–124, 1–18. https://doi.org/10.1016/j.jmarsys.2013.04.002
- Yu, L., & Gan, J. (2022). Reversing impact of phytoplankton phosphorus limitation on coastal hypoxia due to interacting changes in surface production and shoreward bottom oxygen influx. Water Research, 212, 118094. https://doi.org/10.1016/j.watres.2022.118094
- Zhang, J., Liu, S. M., Ren, J. L., Wu, Y., & Zhang, G. L. (2007). Nutrient gradients from the eutrophic Changjiang (Yangtze river) estuary to the oligotrophic Kuroshio waters and re-evaluation of budgets for the East China Sea. *Progress in Oceanography*, 74(4), 449–478. https://doi.org/10.1016/j.pocean.2007.04.019
- Zhang, Y., Lin, X., Shi, X., Lin, L., Luo, H., Li, L., & Lin, S. (2019). Metatranscriptomic signatures associated with phytoplankton regime shift from diatom dominance to a dinoflagellate bloom. Frontiers in Microbiology, 10(590). https://doi.org/10.3389/fmicb.2019.00590
- Zhao, Y., Yu, R. C., Kong, F. Z., Wei, C. J., Liu, Z., Geng, H. X., et al. (2019). Distribution patterns of picosized and nanosized phytoplankton assemblages in the East China Sea and the Yellow Sea: Implications on the impacts of Kuroshio intrusion. *Journal of Geophysical Research: Oceans*, 124(2), 1262–1276. https://doi.org/10.1029/2018JC014681
- Zhou, L., Wu, S., Gu, W., Wang, L., Wang, J., Gao, S., et al. (2021). Photosynthesis acclimation under severely fluctuating light conditions allows faster growth of diatoms compared with dinoflagellates. *BMC Plant Biology*, 21(1), 164. https://doi.org/10.1186/s12870-021-02902-0
- Zhou, W., Yin, K., Long, A., Hui, H., Huang, L., & Zhu, D. (2012). Spatial-temporal variability of total and size-fractionated phytoplankton biomass in the Yangtze River Estuary and adjacent East China Sea coastal waters, China. *Aquatic Ecosystem Health and Management*, 15(2), 200–209. https://doi.org/10.1080/14634988.2012.688727
- Zhou, Z. X., Yu, R. C., Sun, C., Feng, M., & Zhou, M. J. (2019). Impacts of Changjiang river discharge and Kuroshio intrusion on the diatom and dinoflagellate blooms in the East China Sea. *Journal of Geophysical Research: Oceans*, 124(7), 5244–5257. https://doi.org/10.1029/2019JC015158

SUN ET AL. 17 of 17